Proceedings Paper:
Tang, D., Evans, M., Briskham, P. et al. (2 more authors) (2018) Modelling and characterisation of a servo self-piercing riveting (SPR) system. In: Journal of Physics: Conference Series. Modern Practice in Stress and Vibration Analysis (MPSVA) 2018, 02-04 Jul 2018, Cambridge, UK. IOP Publishing .

https://doi.org/10.1088/1742-6596/1106/1/012021

eprints@whiterose.ac.uk
https://eprints.whiterose.ac.uk/

PAPER • OPEN ACCESS

Modelling and Characterisation of a Servo Self-Piercing Riveting (SPR) System

View the article online for updates and enhancements.
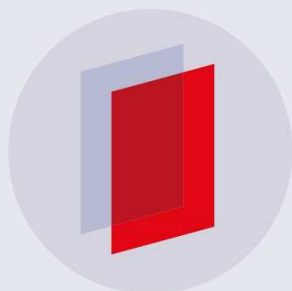
IOP ebooks™

Bringing you innovative digital publishing with leading voices to create your essential collection of books in STEM research.

Start exploring the collection - download the first chapter of every title for free.

Modelling and Characterisation of a Servo Self-Piercing Riveting (SPR) System

D Tang[1,4], M Evans[2], P Briskham[2], L Susmel[3] and N Sims[1]

[1] Department of Mechanical Engineering, The University of Sheffield, 36-38 Victoria Street, Sheffield, S3 7QB, UK

[2] Henrob Ltd., Second Avenue, Zone 2, Deeside Industrial Park, Flintshire, CH5 2NX, UK

[3] Department of Civil and Structural Engineering, The University of Sheffield, Mappin Street, Sheffield, S1 3JD, UK

[4] Author to whom any correspondence should be addressed

E-mail: dhtang1@sheffield.ac.uk

Abstract. SPR is a cold mechanical joining process in which multiple sheets of material are riveted together without the need for a predrilled hole. It works by pushing a typically semi-tubular rivet into a target stack of material, during which the plastic deformation of the material and rivet are such that a mechanical lock is formed within the material stack. The process is used extensively in the automotive industry in car body construction, and is a competing technology to more established joining techniques such as resistance spot welding. As part of the ongoing development of the technique, there is a strong need to understand and simulate the dynamics of the process. In this work, a lumped parameter model of the SPR system with a non-parametric model of the joint is presented. Simulated results are compared with experimental data for a given joint configuration. Furthermore, the model is used to highlight the significance of the compliances within the system. It is shown that during rivet insertion, the stiffness of the C-frame structure is an influential factor in determining the dynamic response of the system. The results provide the basis for a more comprehensive sensitivity analysis into the factors which affect the quality of the resulting joint.

1. Introduction

Self-piercing riveting (SPR) is a cold mechanical joining process in which multiple sheets of material are riveted together without the need for a predrilled hole. It works by punching a typically semi-tubular rivet into a target stack of material, during which the plastic deformation of the material and rivet are such that a mechanical lock is formed within the material stack. The rivet does not typically fully pierce the bottom sheet of material, and in many joint designs does not protrude above the top surface. The typical riveting sequence can be visualised in figure 1(a) and a diagram of a SPR setter assembly is shown in figure 1(b).

In the servo SPR process, the upsetting force required to form the joint is provided by the C-frame structure. The punch is actuated by a servo motor via a roller screw mechanism. The initial velocity of the punch is controlled to determine the amount of kinetic energy input into the joining process.

SPR is used extensively in the automotive industry in car body construction as it offers many advantages over traditional joining techniques such as resistance spot welding [1]. Car manufacturers are increasingly using novel materials which are stronger, lighter, but also more difficult to join. These

new demands often represent a rise in the loads, stresses, and operating speeds of the fastening equipment. There is a growing necessity for model-based analysis and design, which can drive further development of the SPR technique and offer insight into the sensitivities of the process, while minimising the amount of experimental effort required.
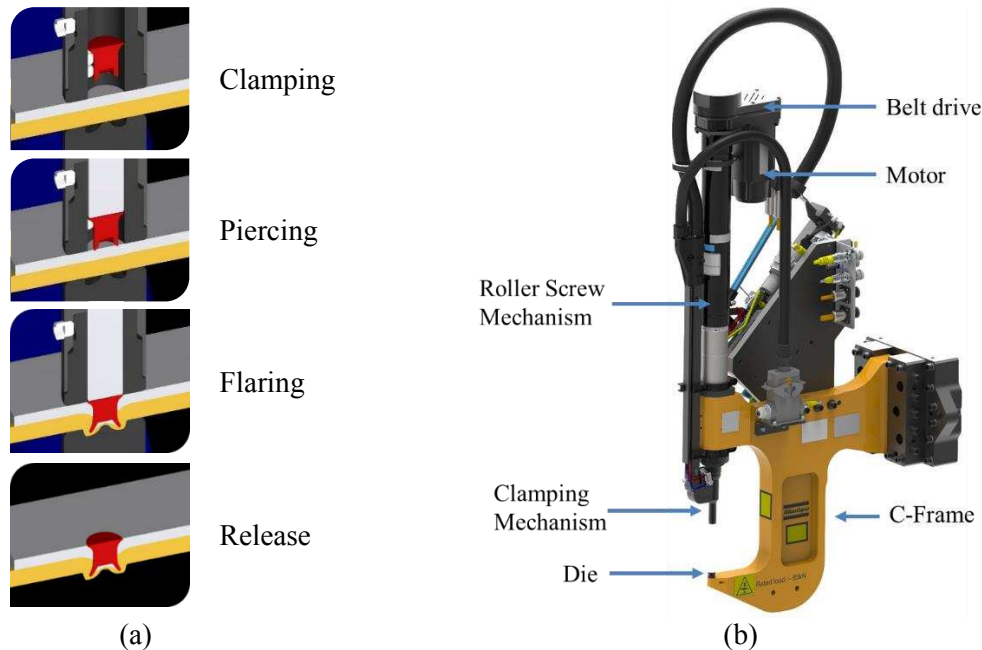
Figure 1. (a) Stages of the rivet insertion process. (b) Illustration of a servo SPR setter assembly.

In the existing literature, the modelling of the SPR process has been predominantly addressed via finite element (FE) methods [2-5]. The number of variables in a typical SPR process makes it a complex subject to model. In [6] Haque compiled a detailed but by no means exclusive list of factors which are known to affect the quality of the joint. However, studies which take a model-based approach to investigating the sensitivity of the process, such as [7] and [8], have focused solely on the interactions at the rivet-material level and do not account for the response of the overall SPR system.

There remains a gap in the existing body of work relating the performance of the full riveting system and the resulting joint. While the effects of the rivet and die properties have traditionally been the subject of investigation, the other components within the system, such as the motor, the mechanical transmission, the C-frame, etc. might have a key influence on the riveting process yet little work has been published in this regard. The knowledge base on SPR would benefit substantially from a comprehensive sensitivity analysis involving the full riveting system.

Works dealing with other joining and forming systems provide useful insight into the identification of models for related processes. The study of a servo-screw press in [9] alluded to the use of force-stroke curves to simulate the dynamic loading of a deep drawing process, and to assess its influence on the drive. In [10], Behrens et al. investigated the interactions between a forming machine and a workpiece, by simulating the respective models separately in their own environments via an "offline-coupling" method. A cold forging press was the subject of investigation in [11], in which the stiffnesses of the press and the tooling were implemented in the FE process simulation as linear spring elements. Parallels can be drawn between the aforementioned processes and the SPR process. The compliances in the SPR system, the model of the workpiece or the joint, and its interaction with the model of the riveting equipment are all critical factors in the accuracy of the simulation.

To better understand the SPR system, it is noted that it is the influence of the machine on the workpiece which is ultimately of interest. A FE approach to the modelling of the SPR system may be

impractical. In contrast, a lumped parameter model is considered more suitable for the purposes of gaining insight into the main dynamics and sensitivities of the process. The mechanical, electrical and digital domains can be easily expressed in a single simulation environment, and furthermore, the low computational cost facilitates iterative analyses. Regarding the model of the joint, it remains to be established if anything short of a full FE model would be capable of representing the joint to the desired level of detail. This paper examines the interaction between an analytical model of the riveting equipment and a non-parametric model of the SPR joint. The model of the SPR process is used to predict the response of the system, and furthermore, to show how the compliances within the system affect its response at the riveting interface.

The structure of this paper is as follows: the next section explains the experimental setup. Then, the modelling of the SPR process is presented. This is followed by results and discussion around the model-based analysis. Ultimately, the conclusions and future work are highlighted.

2. Test Setup

The test rig consists chiefly of a servo SPR setter assembly, as illustrated in figure 1(b). Data are collected on various data loggers and synchronised in post-processing. Measurements are taken on a cycle-by-cycle basis, with each cycle being a full sequence of advance, rivet insertion, and retraction of the punch. The main measurements are as follows: angular velocity and displacement of the motor, relative velocity and displacement between the punch and die, the process force and the motor current.

Due to lack of direct visibility of the rivet during the insertion process, the insertion of the rivet into the stack of material is inferred from the motion of the punch relative to the die, which is observed using a high speed camera. It is assumed that the interface between the punch and the rivet head, as well as the bottom sheet of material and the die remain in contact throughout the loading part of the riveting process. The process force is measured using a load cell located below the die.

3. Modelling

The SPR process was considered as three major subsystems: the Control Unit, the Setter Assembly and the Joint. An illustration of the model is presented in figure 2.
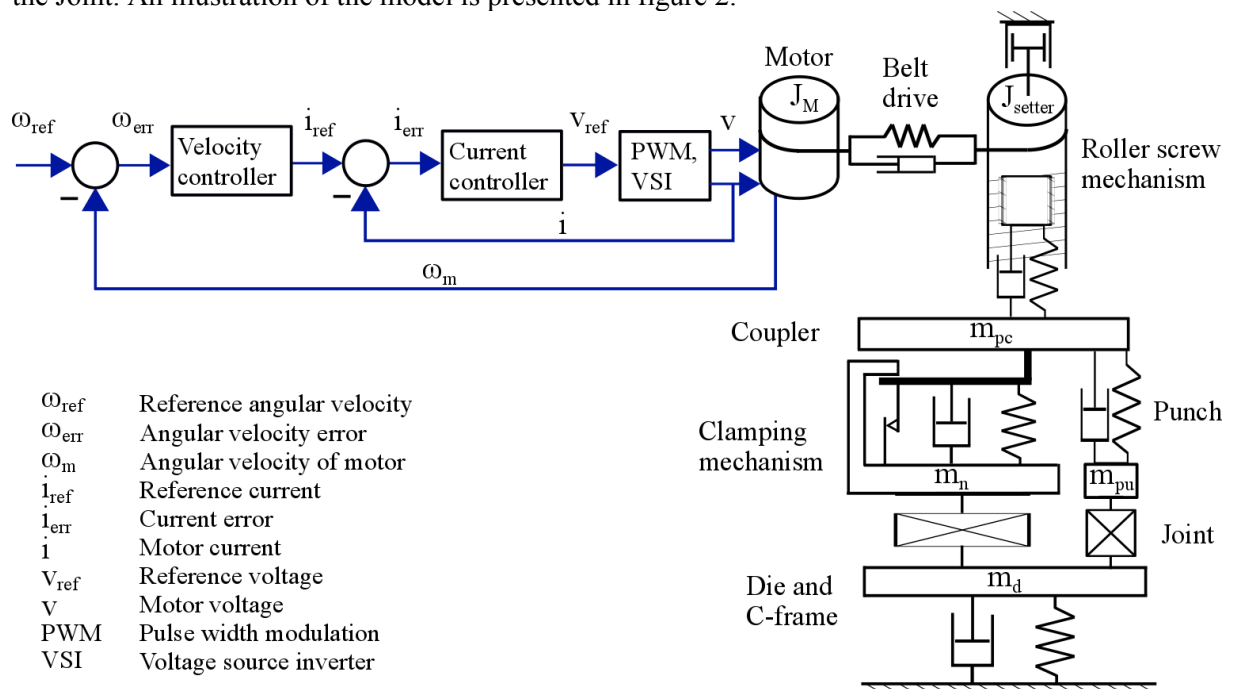
Figure 2. Sketch of the model structure of the system. The control structure is shown on the left with arrows indicating the signal flow, and the setter assembly is shown on the right.

3.1. Setter assembly

The riveting machine was simplified to a six degree-of-freedom system. The model was developed in MATLAB/Simulink via a physics-based approach, in which equations of motion were derived from first principles, and parameter values were either obtained from datasheets or identified experimentally.

The governing equation for the motor is expressed as:

$$J_M \ddot{\theta}_m = T_e - R_1{}^2 K_b \left(\theta_m - \frac{R_2}{R_1} \theta_L \right) - R_1^2 C_b \left(\dot{\theta}_m - \frac{R_2}{R_1} \dot{\theta}_L \right) \tag{1}$$

Where J_M is the inertia of the motor and pulley, θ_m is angular displacement of the motor, T_e is the electromagnetic torque, R_1 and R_2 are the radii of the driving and driven pulleys respectively, K_b is the belt stiffness, θ_L is the angular displacement of the driven pulley, and C_b is the belt damping constant.

Equation (2) describes the dynamics of the roller screw mechanism.

$$\begin{aligned} J_{\text{setter}} \ddot{\theta}_L = {}& R_1 R_2 K_b \left(\theta_m - \frac{R_2}{R_1} \theta_L \right) + R_1 R_2 C_b \left(\dot{\theta}_m - \frac{R_2}{R_1} \dot{\theta}_L \right) \\ & - \left(\frac{F_L P_h}{2\pi} + \text{sign}(\dot{\theta}_L) \frac{F_L D_0}{2} \mu_{\text{prac}} + B_r \dot{\theta}_L \right) \end{aligned} \tag{2}$$

Where J_{setter} is the inertia of the rivet setter, P_h is the lead of the roller screw, D_0 is the nominal diameter of the nut, μ_{prac} is the coefficient of friction, and B_r is the viscous friction coefficient. F_L is the force transmitted axially through the shaft of the roller screw during the riveting operation, defined as:

$$F_L = K_r (x_r - x_{\text{pc}}) + C_r (\dot{x}_r - \dot{x}_{\text{pc}}) \tag{3}$$

Where K_r and C_r are the effective stiffness and damping constants of the roller screw, x_r is the axial displacement of the roller assembly, and x_{pc} is the displacement of the coupler. The coupler connects the output shaft of the roller screw mechanism to the punch and is also a critical component in the generation of the clamping force. The governing equation for the coupler is formulated as:

$$m_{\text{pc}} \ddot{x}_{\text{pc}} = F_L - K_{\text{plpu}}(x_{\text{pc}} - x_{\text{pu}}) - C_{\text{plpu}}(\dot{x}_{\text{pc}} - \dot{x}_{\text{pu}}) - F_{\text{clamp}} \tag{4}$$

Where m_{pc} is the mass of the coupler, K_{plpu} is the effective stiffness of the plunger-punch subassembly, x_{pu} is the displacement of the end of the punch, and C_{plpu} is the effective damping in the plunger-punch subassembly. F_{clamp} is the clamping force applied by the clamping tube on the stack of material, and is dependent on the relative motion between the coupler and the clamping tube. The details are not included here due to limited space.

The dynamics of the clamping tube are described by:

$$m_n \ddot{x}_n = F_{\text{clamp}} - r_{\text{mat}} \tag{5}$$

Where m_n is the mass of the clamping tube and $\ddot{x}_n$ is its acceleration. r_{mat} is the restoring force of the material stack under compression, which is defined in section 3.2.

The riveting force r is transmitted directly through the plunger-punch subassembly, which is treated as a single component. Its equation of motion is expressed as:

$$m_{\text{plpu}} \ddot{x}_{\text{pu}} = K_{\text{plpu}}(x_{\text{pc}} - x_{\text{pu}}) + C_{\text{plpu}}(\dot{x}_{\text{pc}} - \dot{x}_{\text{pu}}) - r \tag{6}$$

Where m_{plpu} is the mass of the plunger-punch subassembly. r is defined in section 3.2.

The C-frame is modelled as mass-spring-damper system, the parameters of which are identified using a high-speed camera. The C-frame and setter are treated as two separate subsystems which interact only via the SPR joint. Equation (7) describes the dynamics of the C-frame.

$$m_{\mathrm{d}}\ddot{x}_{\mathrm{d}} = r + r_{\mathrm{mat}} - K_{\mathrm{c}}x_{\mathrm{d}} - C_{\mathrm{c}}x_{\mathrm{d}} \tag{7}$$

Where x_{d} is the displacement or deflection of the C-frame.

3.2. SPR joint

The modelling of the SPR joint was framed as a nonlinear system identification problem, to which the restoring force surface (RFS) method was well suited. The technique as described in [12] and its variant in [13], were used as a reference in the development of the model. The individual responses of the system to multiple riveting cycles were collected into a single dataset representing its response to a series of impulse excitations.

Regarding its interactions within the full system model, the joint was considered as a nonlinear element which generated a restoring force according to the extent and rate of its compression, i.e. the displacement and velocity across the nonlinear element, or the punch-die relative displacement.

Variations of the model of the joint were evaluated:
1. The RFS as a three dimensional surface, shown in figure 3(a).
2. A two dimensional polynomial curve defined in force vs. displacement, shown in figure 3(b).
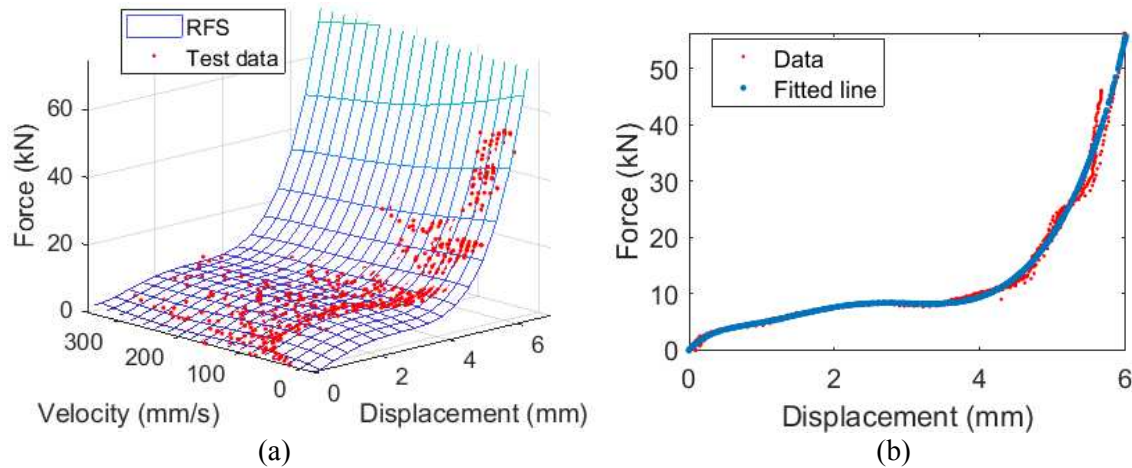
Figure 3. (a) Restoring force surface. (b) Force-displacement characteristic.

With reference to figure 3(b), the velocity dependence of the given joint configuration was assumed to be negligible, based on the repeatability of the force-displacement profiles across the range of setting velocities $100 – 300$ mm/s. Therefore, for characterising the given joint configuration, the simpler model defined in force-displacement was considered adequate. The riveting force r was defined as a seventh-order polynomial function f:

$$r = \mathrm{f}(x_{\mathrm{pu}} - x_{\mathrm{d}}) \tag{8}$$

The restoring force of the material under clamping was defined as:

$$r_{\mathrm{mat}} = K_{\mathrm{mat}}(x_{\mathrm{n}} - x_{\mathrm{d}}) + C_{\mathrm{mat}}(\dot{x}_{\mathrm{n}} - \dot{x}_{\mathrm{d}}) \tag{9}$$

Where K_{mat} is the effective stiffness of the material, x_{n} is the displacement of the clamp tube, and C_{mat} is the effective damping constant of the material.

4. Results and Discussion

4.1. Simulated riveting process

The performance of the full model was assessed via the comparison of experimental and simulated data. Figure 4(a) shows the punch-die relative displacement and force traces for the loading part of a riveting

process. Figure 4(b) shows the relative velocity and force from the same run plotted against the relative displacement. The relative displacement represents the extent of rivet insertion into the material, and the relative velocity represents the rate of rivet insertion.
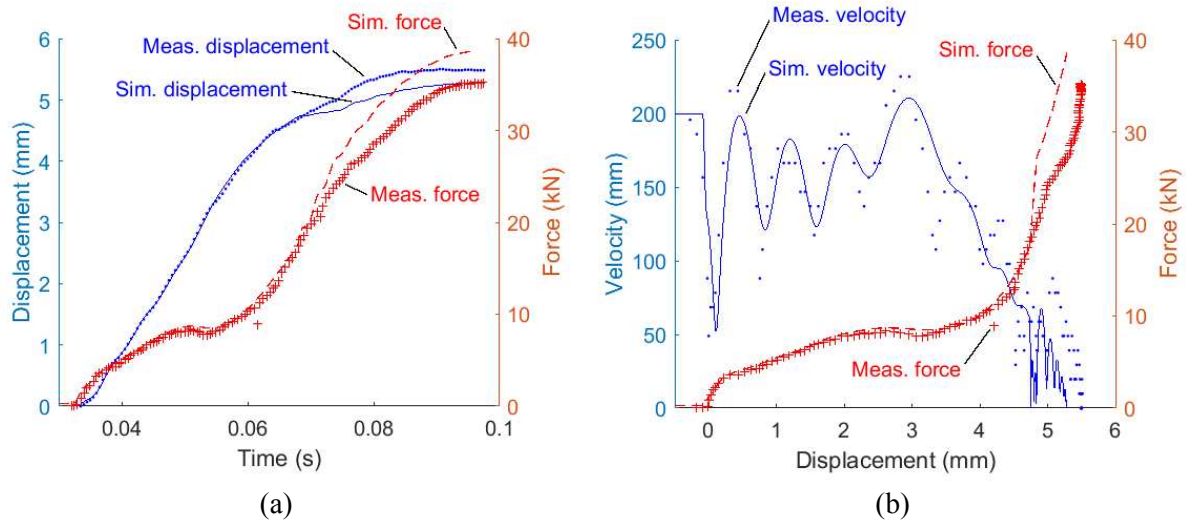
Figure 4. Comparison between simulated and experimental data, (a) Relative displacement and force vs. time, (b) Relative velocity and force vs. relative displacement.

Good agreement in the results are observed up to 0.07 s in time or 4.5 mm in displacement, at which point the simulated traces start to deviate from the experimental data. The issue can be attributed to two main factors: firstly, the behaviour of the material under the clamping load was not adequately modelled, leading to a faster build-up of clamping force through the riveting process. Secondly, the rivet insertion was characterised using the total process force rather than the actual force transmitted through the rivet, hence the simulated riveting force was larger than desired, leading to the simulated total force being higher than that observed experimentally.

In order to improve the performance of the model, the direct measurements of either the riveting force or the clamping force are necessary. Knowing either component of the total process force will allow the other to be calculated. Better characterisation of the material behaviour under clamping would further improve the accuracy of the model.

4.2. Model-based analysis of the effects of the C-frame stiffness

The effect of the static and dynamic properties of the C-frame on the joint was of particular interest. The effective stiffness of the C-frame model was varied to examine how the changes influenced the punch-die relative motion. Three different values were chosen to represent a low, intermediate and high stiffness in the range of stiffnesses of real C-frame types. All other variables in the simulation were kept the same, including the process parameters and the joint configuration. The simulated results are shown in figure 5.

From figure 5(a) it can be seen that at the given setting velocity, the stiffness of the C-frame has a notable effect on the process force. The maximum force increases with C-frame stiffness, which is not surprising when considering the conversion of the kinetic energy of the setter into stored strain energy of the C-frame. In figure 5(b) the traces represent the extent of the simulated rivet insertion. The overall displacement increases for C-frames of larger stiffnesses, as a consequence of the larger process force generated. In figure 5(c), up to 0.055 sec, the oscillatory response of the punch relative to the die is due to the initial riveting load. Taking the case of the intermediate stiffness, K_c:136646000 N/m, the frequency of the initial oscillations is 200 Hz, which matches the natural frequency of the C-frame. The oscillation of the C-frame implies oscillation of the die, which is expected to directly affect the forming of the joint and the joint quality. The results strongly suggest that the dynamics of the C-frame dominate

the response of the system at the riveting interface, and therefore significantly influence the rivet insertion process.
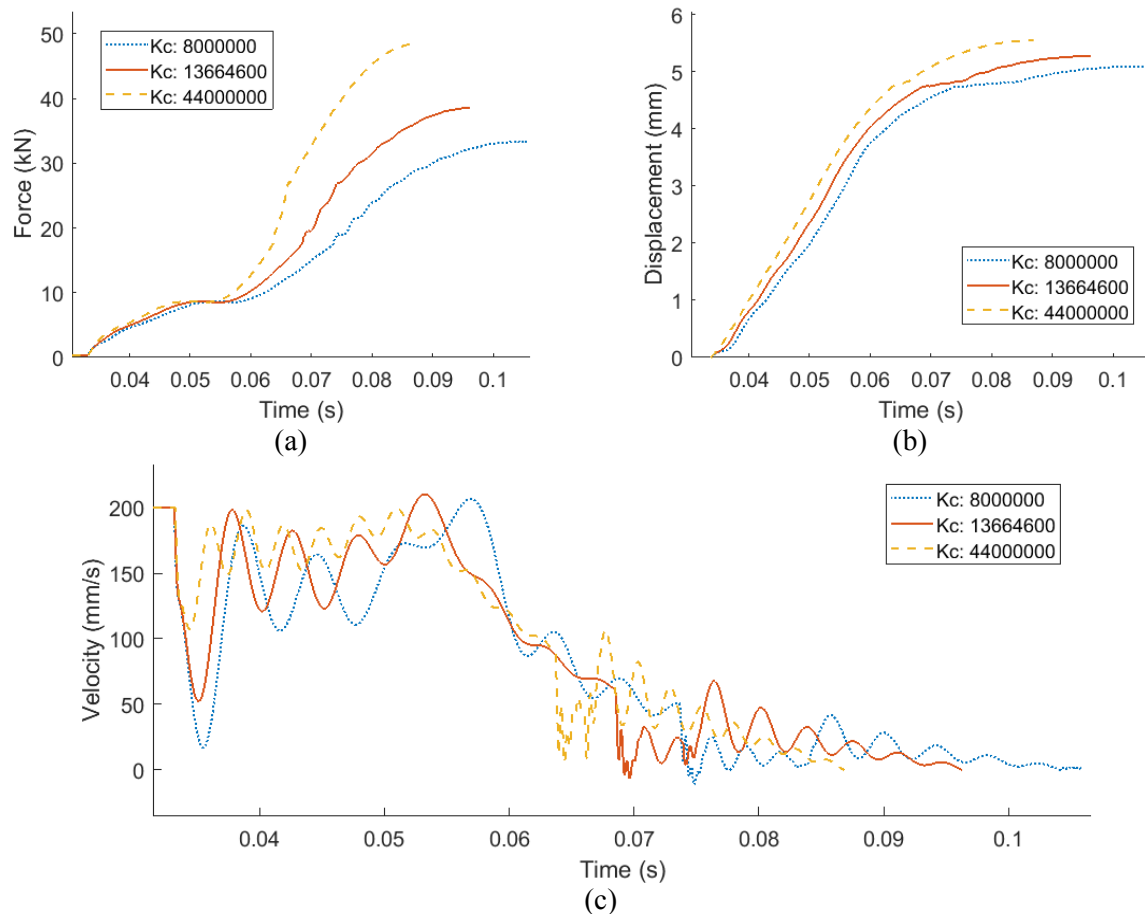
Figure 5. Effects of changing the effective stiffness K_c of the C-frame. (a) Force vs. time, (b) Relative displacement vs. time, (c) Relative velocity vs. time.

In light of the results, a question is raised over the one of the underlying assumptions in the modelling of the joint: that the force-displacement characteristic curve for the joint was independent of the compliance of the system on which it was identified. Having argued that the dynamics of the C-frame significantly influence the riveting process, it can also be argued that the characterisation of a joint configuration on a particular system may yield a model which is specific to that system. Further joint identification on different C-frame types is required to verify the validity of the assumption.

The current study may have implications for the body of work relating to the FE-based modelling of the SPR process, in which the dynamic response of the riveting machine and C-frame are broadly unaccounted for. These approaches may be representative of the SPR process on traditional hydraulic systems, where the mode of rivet insertion can be considered as quasi-static loading. However, in the case of inertia-based servo systems the inertial effects are believed to play an important role, and therefore should be included in modelling of the process.

5. Conclusion

A lumped parameter model of the SPR process has been created in MATLAB/Simulink.

The simulated response of the system has been compared against experimental results for a given joint configuration. Partial agreement indicates that dynamics in the riveting system have been suitably

captured in the model during the initial phase of rivet insertion. Assuming that the force-displacement characteristic of the joint is not affected by the compliance of the system on which it is identified, the simulated results suggest that the dynamic response of the machine at the riveting interface is significantly influenced by the dynamics of the C-frame.

Further work should be focused on the identification of the different components of the total process force, and also characterisation of different types of C-frames in order to validate the results of the model-based analysis. Another area of interest would be how the dynamics of the C-frame affect the quality of the joint. The findings of this work form the basis for a more comprehensive sensitivity analysis of the servo SPR system.

Acknowledgements

References

[1]   Briskham P, Blundell N, Han L, Hewitt R, Young K and Boomer D 2006 Comparison of Self-Pierce Riveting, Resistance Spot Welding and Spot Friction Joining for Aluminium Automotive Sheet (SAE International)
[2]   Bouchard P-O, Laurent T and Tollier L 2008 Numerical modeling of self-pierce riveting—from riveting process modeling down to structural analysis *J. Mater. Process. Technol.* **202** 290-300
[3]   Casalino G, Rotondo A and Ludovico A 2008 On the numerical modelling of the multiphysics self piercing riveting process based on the finite element technique *Adv. Eng. Softw.* **39** 787-95
[4]   Porcaro R, Hanssen AG, Langseth M and Aalberg A 2006 Self-piercing riveting process: An experimental and numerical investigation *J. Mater. Process. Technol.* **171** 10-20
[5]   Huang L, Moraes JFC, Sediako DG, Jordon JB, Guo H and Su X 2016 Finite-Element and Residual Stress Analysis of Self-Pierce Riveting in Dissimilar Metal Sheets *J. Manuf. Sci. Eng.* **139** 021007
[6]   Haque R 2018 Quality of self-piercing riveting (SPR) joints from cross-sectional perspective: A review *Arch. Civ. Mech. Eng.* **18** 83-93
[7]   Mucha J 2011 A study of quality parameters and behaviour of self-piercing riveted aluminium sheets with different joining conditions *Strojniški vestnik-J. Mech. Eng.* **57** 323-33
[8]   Jäckel M, Falk T and Landgrebe D 2016 Concept for Further Development of Self-pierce Riveting by Using Cyber Physical Systems *Procedia CIRP* **44** 293-7
[9]   Schenke C-C, Wiemer H and Großmann K 2012 Analysis of servo-mechanic drive concepts for forming presses *Prod. Engineer.* **6** 467-74
[10] Behrens B-A, Bouguecha A, Krimm R, Matthias T and Czora M 2013 Consideration of the Machine Influence on Multistage Sheet Metal Forming Processes *Process Machine Interactions*, ed Denkena B, Hollmann F (Berlin: Springer-Verlag Berlin Heidelberg) pp 403-17
[11] Kroiß T, Engel U and Merklein M 2013 Comprehensive approach for process modeling and optimization in cold forging considering interactions between process, tool and press *J. Mater. Process. Technol.* **213** 1118-27
[12] Masri S and Caughey T 1979 A nonparametric identification technique for nonlinear dynamic problems *J. Appl. Mech.* **46** 433-47
[13] Crawley EF and Aubert AC 1986 Identification of nonlinear structural elements by force-state mapping *AIAA J.* **24** 155-62